Performance of a small air-lift pump

D. A. Kouremenos and J. Staïcos*

Pumping of liquids using two-phase flow has been examined experimentally in small air-lift pumps with 12–19 mm bore plexiglass tubes. An air injection system was devised to create and maintain 'perfect' slug flow in the vertical riser tube. An equation has been derived, based on momentum conservation considerations, which correlates well with the measurements obtained. Slip variation, or liquid holdup, between the two phases and the formation of the 'entrance' section part of the pump (suction pipe) were taken into consideration. Unlike its predecessors, this equation predicts the reversal in the pump performance curve observed experimentally.

Keywords: *two-phase flow, air-lift pumps*

Numerous studies have been published relating to the interpretation and analysis of air-lift pump performance, usually dealing with pumps having considerable depth of submergence and height of discharge. Little information is available on pumps with small submergence, discharge and diameter. In addition, little has been reported on the effect of the formation of the 'entry region' (suction pipe) of the pump or of the injection system (injector) on pump performance[1–7].

All published theoretical analyses of air-lift pumps have been based on slug two-phase flow. The experimental results presented in those studies, however, are not the output of a constant and perfect slug flow but from a 'composite' flow, starting as bubbly flow and ending as annular flow.

The work described here is a contribution to the study of the performance of small air lift pumps, for constant perfect slug two-phase flow. Specifically, four small test pumps were made from Plexiglass tubes of standard length ($L = 933$ mm) and with 12.00, 14.50, 16.00 and 19.23 mm bores.

Air was injected at the entrance of the riser using on-axis copper tubes of smaller diameter than the Plexiglass tubes. Appropriate valves of the same form and different dimensions were installed at the end of the copper tubes, thus forming the injector. The valves were operating by the pressure of the air provided to the pump.

Four copper tubes with different external diameters and valves of corresponding dimensions were used. Since the air supply tubes are inserted coaxially in the Plexiglass tubes of the pump, a suction pipe of length $t_s = 98$ mm was created (Fig 3). The cross-sectional area (annular) of the suction pipe corresponds to the difference $(D-d)$ of the two tube diameters.

A control system, in the air supply circuit, operating with constant frequency, interrupts the air flow to the injector. The resulting opening and closing of the air valve creates perfect and constant slug flow regime in the riser. This flow regime was maintained during all the experiments.

For each combination of pump and air supply tube, measurements were made for various submergence ratios. Specifically, volumetric flow rate of the water (Q_w) was measured for different air flow rates (Q_a). Factors related to each measurement are bore of riser D, external diameter of the air supply tube d, their ratio $\xi = (D/d)$, and the submergence ratio $\beta = (t/l)$.

Experimental apparatus

The experimental apparatus is shown in Fig 1. The pump is formed by a Plexiglass tube of length $K = 933$ mm located vertically at the centre of a $1000 \times 500 \times 500$ mm Plexiglass water tank. Tubes with four different internal diameters D ($D = 12.00$, 14.50, 16.00, 19.23 mm) were used in the experiments.

Air supply copper tubes with the appropriate injection valves were located coaxially inside the corresponding pump tubes for a length $t_s = 98$ mm (suction pipe). With this arrangement an annular section, along the length of the suction pipe, was created in each case having thickness $(D-d)$ and length $t_s = 98$ mm. The remainder of the tube, having standard length $(l = L - t_s)$ is the riser or discharge pipe. Fig 2 is a cross-section of the form of the air injection valve. Its dimensions depend on the diameter of the air-supply tubes.

The pumped water did not return to the initial water tank but flowed either to a storage tank or to a volume measuring receiver. A separate header tank ensured a constant level in the water tank during each test.

An air control system interrupted air flow to the injector at a constant, adjustable frequency. This controlled opening and closing of the air injection valve produced large bubbles (slug flow). The volumetric flow rate of air was measured, after leaving the riser, using a wet-type gas meter. Gauge pressure of the air in the air-supply tubes and near the air injection valve was ensured with a water manometer. Micromanometers were used at the exit of the riser and at the entrance of the wet-type gas meter. Except for the measuring receiver and wet-type gas

* National Technical University of Athens, Mechanical Engineering Department, Thermal Section, 42 Patission Street, 106 82 Athens, Greece
Received 24 May 1984 and accepted for publication in final form on 18 March 1985

meter, an electrical chronometer was used in measuring the volumetric flow rate of air and water.

Basic equation

Consider the air-lift pump system as shown in Fig 3. $l=t+h$ is the riser or discharge pipe, while the remainder, t_s, is the suction pipe. When air, at an appropriate flow rate, is injected into the riser through the injection-valve, at depth t below water level, water is pumped up to the discharge at height h at a rate Q_w.

Applying conservation of momentum to the control surface (shown in Fig 3 by a dotted line) under steady operating conditions:

$$\beta-\bar{E}_w=\frac{V_{wo}^2}{2gl}(\sigma_1+\sigma_2+\sigma_3) \quad (1)$$

where σ_1, σ_2, σ_3, are dimensionless quantities expressing the losses in: (1) the riser (two-phase flow) (2) the injection-valve and (3) the suction pipe. They are:

$$\sigma_1=\bar{E}_w^{1.7}\lambda_0(l/D) \quad (2)$$

$$\sigma_2=W_3\left(1+\frac{Q_\alpha}{Q_w}\right)\frac{\xi^2}{\xi^2-1} \quad (3)$$

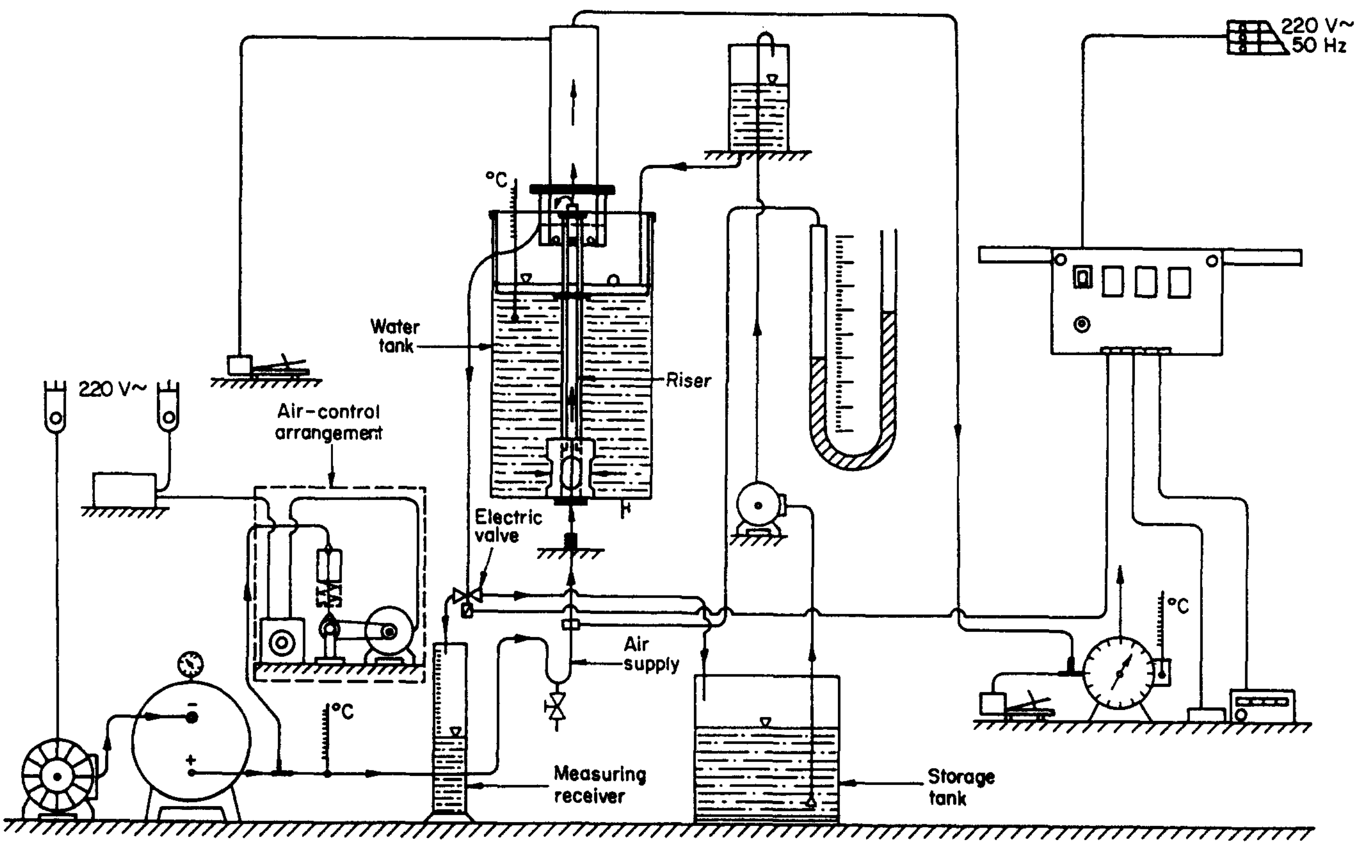

Fig 1 Test apparatus

Notation

A_0,A_δ	Cross-sectional area of pipe and annular suction pipe respectively
d	External diameter of air injection tube
D	Pipe diameter
$\bar{E}$	Average holdup
f	Friction factor defined by head loss $(4flV^2)/(2gD)$
g	Gravitational acceleration
h	Height of discharge
k	Friction parameter, $(4fl/D)$
l	Length of riser, $h+t$
L	Length of pump tube, $l+t_s$
Q	Volume flow rate
s	Slip ratio, $(Q_\alpha/Q_w)(\bar{E}_w/\bar{E}_\alpha)$
t	Depth of submergence
t_s	Length of suction pipe
$V_{(\ )0}$	Superficial velocity in pipe, Q/A_0
W_3	Coefficient of losses in injector region
β	Submergence ratio, t/l
ξ	Diameter ratio, D/d
λ_0	Friction factor based on liquid single phase flow
λ_δ	Friction factor in annular suction pipe (single phase flow)
σ_1,σ_2,σ_3	Coefficients
$\Phi(D/d)$	Coefficient

Subscripts

l	Liquid
g	Gas
w	Water
α	Air

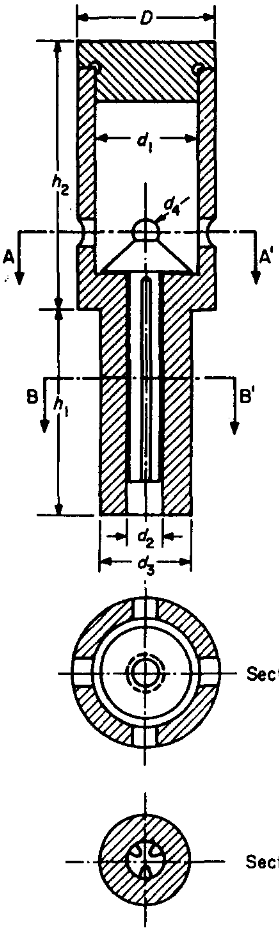

Valve dimensions						
D (mm)	d_1 (mm)	d_2 (mm)	d_3 (mm)	d_4 (mm)	h_1 (mm)	h_2 (mm)
8.0	7.0	3.0	6.0	3.5	33.0	25.0
10.0	9.0	4.0	7.8	5.0	33.0	26.0
12.0	10.5	5.0	9.7	6.0	32.0	24.0
14.0	12.0	6.0	12.0	6.5	30.0	25.0
16.0	14.5	6.0	13.7	7.0	32.0	25.0

Fig 2 Cross-section of the air injection valve

$$\sigma_3=\lambda_\delta\frac{t_s}{D-d}\left(\frac{\xi^2}{\xi^2-1}\right)^2 \quad (4)$$

More details are given in the Appendix.

Results and discussion

Flow regime

Perfect slug two-phase flow was maintained in all cases examined.

Discharge characteristics

Characteristic curves $Q_w=f(Q_\alpha)$ were obtained. Specifically, for each of the four risers, four families of curves were obtained using the four air-supply tubes with different diameters in each riser.

Each family includes characteristics corresponding to four submergence ratios ($\beta=0.70$, 0.65, 0.60, 0.55) for D, ξ constant. Hence, 16 characteristics were obtained for each riser.

Figs 4 and 5 show two families of characteristics for two risers ($D=12.00$, 19.23 mm) and $\xi=\xi_{max}$. Figs 6–9 are non-dimensional plots of four families of characteristics corresponding to the four risers and for $\xi=\xi_{max}$, according to the equation:

$$Q_w/(A_0(2gl)^{1/2})=f(Q_w/Q_\alpha)$$

These figures demonstrate that Eq (1) correlates well with the experimental results. Particularly, the dimensionless plot leads to the conclusion that this equation predicts successfully the reversal of the curves at low air flow rates, as well as the point of minimum (Q_α/Q_w) is encountered (maximum efficiency).

Comparison with the Stenning and Martin model

For the simulation of air-lift pump performance, Stenning and Martin[8] proposed the relation:

$$(t/l)-\left(1\Big/\left(1+\frac{Q_g}{sQ_l}\right)\right)=\left(\frac{V_{fo}^2}{2gl}\right)\left((k+1)+(k+2)\left(\frac{Q_g}{Q_l}\right)\right) \quad (5)$$

where

$k=4f(l/D)$ (friction parameter)

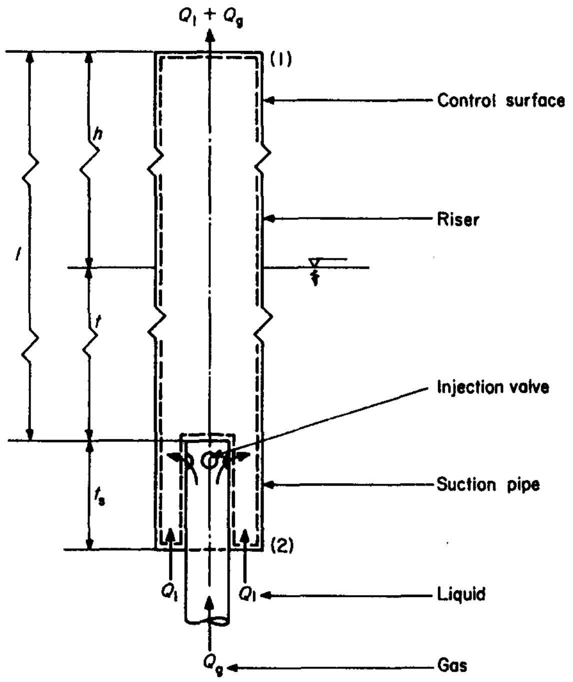

Fig 3 Analytical model of air-lift pump

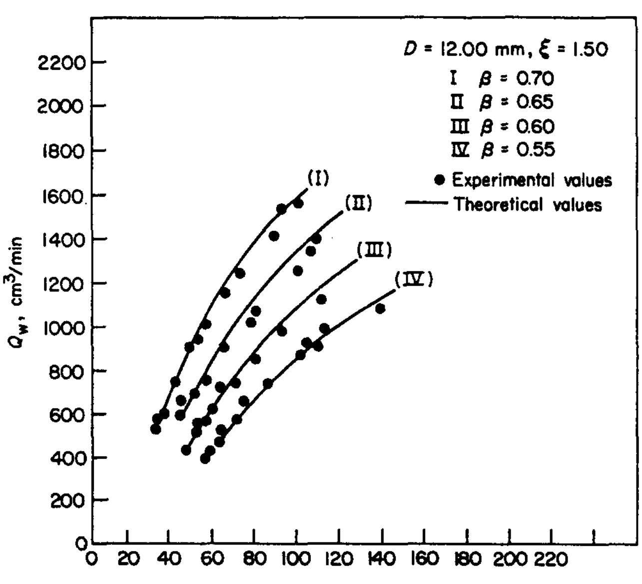

Fig 4 Relationship between volumetric flow rate of water discharge and air supplied for D = *12.00 mm*

and:

$$s=\frac{Q_g}{Q_l}\frac{\bar{E}_l}{\bar{E}_g} \qquad \text{(slip ratio)}$$

are fixed values.

Here air-lift pump performance has been simulated by Eq (1) which has the advantage that the friction parameters λ_0, λ_δ, W_3 and slip ratio s (or $\bar{E}_1$) are variable depending on the flow rates $Q_g(Q_\alpha)Q_l(Q_w)$. A consequence of this novelty is that the present equation gives more realistic predictions than Eq (5). Fig 9 shows that Eq (5) fails to predict the reversal of the $V_{wo}/(2gl)^{1/2}=f(Q_\alpha/Q_w)$ curve, while Eq (1) predicts this behaviour. This reversal has been observed experimentally in this study (Figs 6–9) as well as in Parker's[10] related measurements.

Conclusions

This study provides the first data on air-lift pumps of small diameters ($D=12.00$ to 19.23 mm). The measurements showed a reversal in the characteristic curve of the pump, which has also been observed by previous workers, but which could not be predicted by the available correlations which use fixed values of the friction parameter and slip ratio. A correlation derived here uses variable values of the above parameters and predicts the experimentally observed reversal of the air-lift pump characteristic curve.

References

1 **Davis G. J. and Weidrer G. R.** An investigation of the air-lift pump. *Bulletin of the University of Wisconsin, 1914,* **6**(*7*), *405–573*

2 **Ward, C. N. and Kessler, L. N.** Experimental study of air-lift pumps and application of results to design. *Bulletin of the University of Wisconsin, 1924,* **9**(*4*), *5–165*

3 **Stepanoff A. J.** Thermodynamic theory of the air-lift pump. *Trans. A.S.M.E., 1929, 49–58*

4 **Pickert F.** The theory of air-lift pumps. *Engineering, July 1932, No 134, 19*

5 **Cattaneo A. G.** Über die Förderung von Flüssgkeiten mittels der eigenen Dampfe. *Zeitschrift für die gesante Kälte-Industrie, 1935,* **42**(*1*)

6 **Cattaneo A. G.** Über die Förderung von Flüssgkeiten mittels der eigenen Dampfe. *Zeitschrift für die gesante Kälte-Industrie, 1935,* **42**, (*3*)

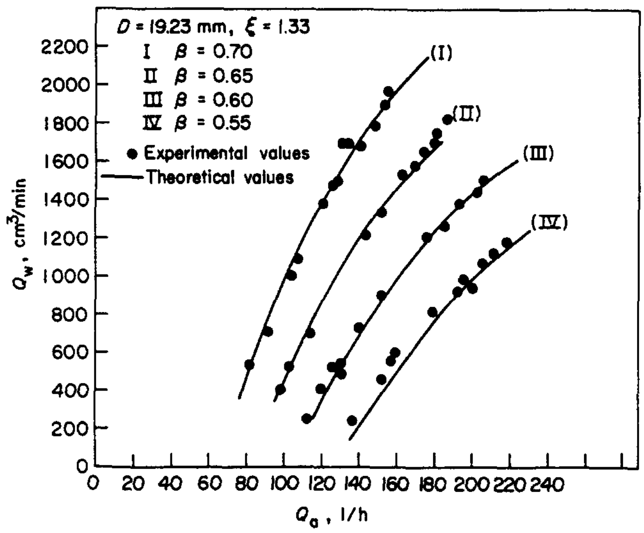

Fig 5 Relationship between volume flow rate of water discharge and air rate supplied for D = *19.23 mm*

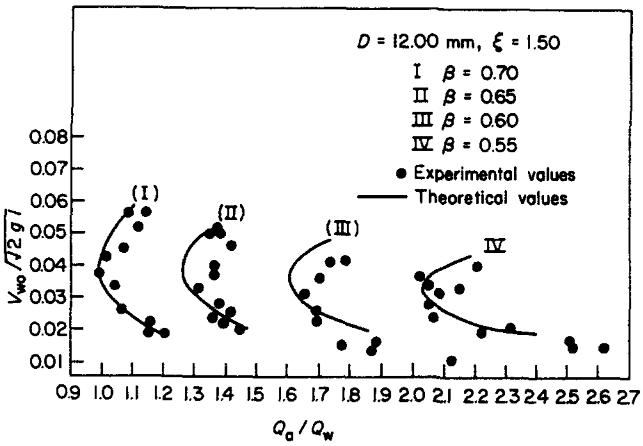

Fig 6 Dimensionless plot of pump performance (D = *12.00 mm*)

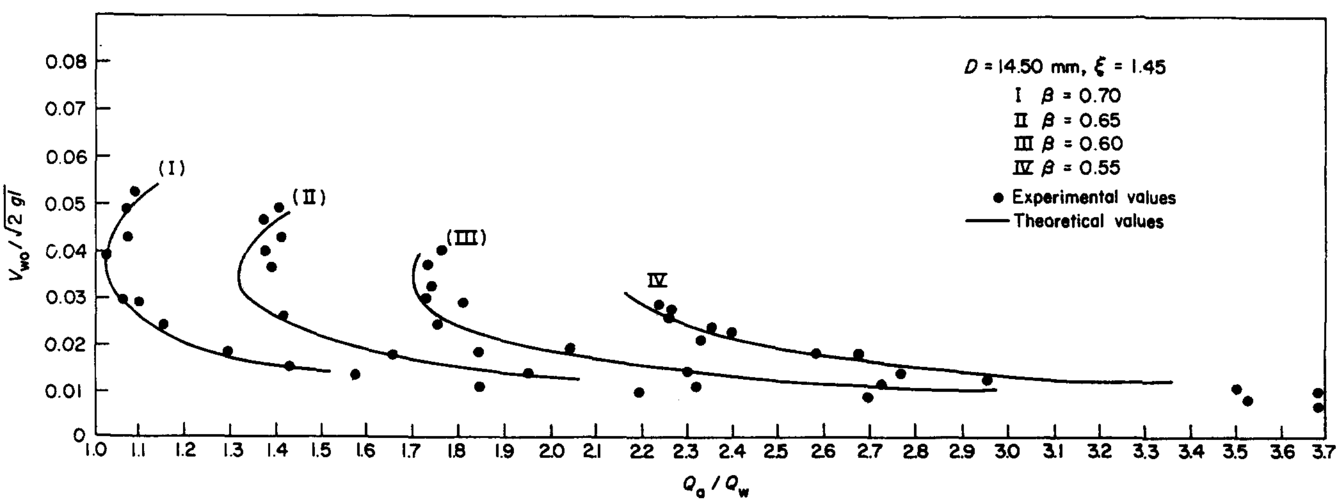

Fig 7 Dimensionless plot of pump performance (D = *14.50 mm*)

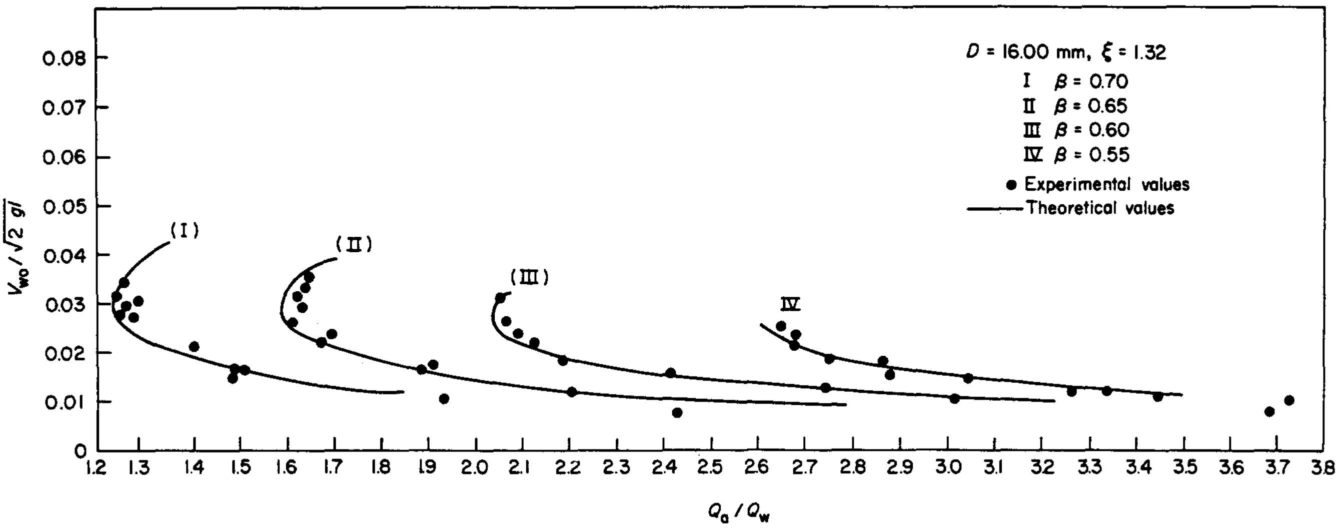

Fig 8 Dimensionless plot of pump performance (D = *16.00 mm*)

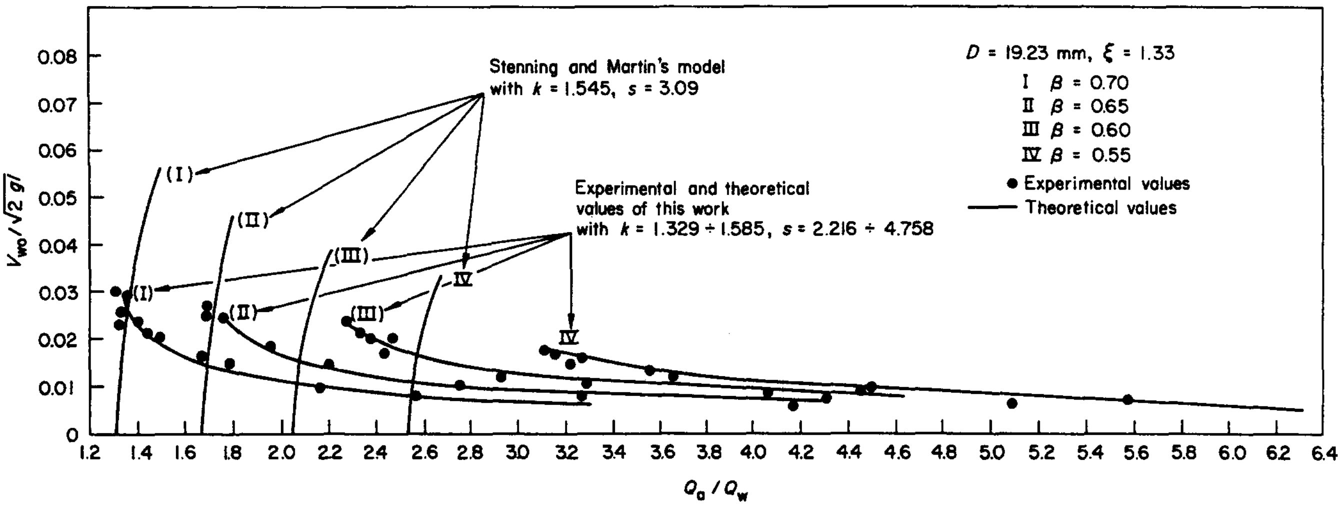

Fig 9 Dimensionless plot of pump performance. Comparison with Stenning and Martin's 'theoretical' model (D = *19.23 mm*)

7 **Nicklin D. J.** The air-lift pump: Theory and optimisation. *Trans. Instn. Chem. Engrs, 1963*, **41**, *29–39*

8 **Stenning A. H. and Martin C. B.** An analytical and experimental study of air-lift pump performance. *J. Engng for Power, Trans. A.S.M.E., April 1968, 106–110*

9 **Todoroki I., Sato Y. and Honda T.** Performance of air-lift pump. *Bull. JSME, April 1973*, **16**(*94*), *733–41*

10 **Parker G. J.** The effect of footpiece design on the performance of a small air-pump. *Int. J. Heat and Fluid Flow, December 1980*, **2**(*4*), *245-252*

11 **Knudsen J. G. and Katz K. L.** Fluid Dynamics and Heat Transfer, *McGraw-Hill Book Company, New York, 1958*

12 **Wallis G. B.** One-dimensional two-phase flow, *McGraw-Hill Book Company, 1969*

13 **Hütte Bd. I.** *Verlag von Wilhelm Ernst & Sohn, Berlin, 1955, 219*

Appendix

Application of a momentum balance to the control volume shown in dotted line in Fig 3 gives:

$$\text{(Rate of momentum change)}_1^2 = \text{(Gravity forces)}_1^2 + \text{(Pressure forces)}_1^2 + \text{(Forces due to the external shear stresses)}_1^2 \quad \text{(A1)}$$

where the quantities in brackets may be calculated from:

$$\text{(Rate of momentum change)}_1^2 = A_0 \rho_l \frac{V_{f0}^2}{2}\left(\left(\frac{\xi^2}{\xi^2-1}\right)^2\right) \quad \text{(A2)}$$

$$\text{(Gravity forces)}_1^2 = -(A_\delta \rho_l g t_s + A_0 \bar{E}_l \rho_l g l) \quad \text{(A3)}$$

$$\text{(Pressure forces)}_1^2 = (A_0 \rho_l g t + A_\delta \rho_l g t_s) - \left((A_0 - A_\delta)\lambda_\delta \frac{t_s}{D-d} \rho_l \frac{V_{f0}^2}{2}\left(\frac{\xi^2}{\xi^2-1}\right)^2\right) \quad \text{(A4)}$$

$$\text{(Forces due to external shear stresses)}_1^2 = -(T_1 + T_2 + T_3 + T_4 + T_5) \quad \text{(A5)}$$

where T_1, T_2, T_3, T_4 and T_5 represent resistances, at the entrance, at the annular part t_s, in the injection area, in the two-phase flow region and at the outlet of the pump p, respectively.

T_1 and T_5 may be neglected due to the low fluid velocity at the inlet and outlet of the pump. The other terms are given by:

$$T_2 = -A_\delta \lambda_\delta \frac{t_s}{D-d} \rho_l \frac{V_{f0}^2}{2}\left(\frac{\xi^2}{\xi^2-1}\right)^2 \quad \text{(A6)}$$

$$T_3 = -A_\delta W_3 \rho_l \frac{V_{f0}^2}{2}\left(1+\frac{Q_g}{Q_l}\right)\left(\frac{\xi^2}{\xi^2-1}\right)^2 \qquad \text{(A7)}$$

$$T_4 = -A_0 \bar{E}_l^{-z} \lambda_0 \frac{1}{D} \rho_l \frac{V_{f0}^2}{2} \qquad \text{(A8)}$$

Inserting these quantities into Eq (A1) and neglecting[7] the term expressing the rate of momentum change, gives, after some manipulation, the dimensionless equation:

$$\beta - \bar{E}_l = \frac{V_{f0}^2}{2gl}(\sigma_1 + \sigma_2 + \sigma_3) \qquad \text{(A9)}$$

where:

$\sigma_1 = \bar{E}_l^{1.7} \lambda_0 (l/D)$ (losses in the riser[9])

$\sigma_2 = W_3\left(1+\frac{Q_g}{Q_l}\right)\frac{\xi^2}{\xi^2-1}$ (losses in the injector)

$\sigma_3 = \lambda_\delta \frac{t_s}{D-d}\left(\frac{\xi^2}{\xi^2-1}\right)^2$ (losses in the suction pipe)

In these expressions the average liquid holdup $\bar{E}_l$ is given[3,4] by:

$$\bar{E}_l = 1 - \bar{E}_g = \frac{V_{f0} + 0.345(gD)^{1/2}}{V_{f0}(1+Q_g/Q_l) + 0.345(gD)^{1/2}} \qquad \text{(A10)}$$

and the friction factors λ_0, λ_δ by:

$\lambda_0 = \frac{64}{Re}$ for $Re_{f0} < 2500$

$\lambda_0 = \frac{0.316}{Re^{0.25}}$ for $Re > 3500$

$\lambda_\delta = \Phi \lambda_0$ for annular section and[11] $Re_{f\delta} < 2500$

The coefficient W_3 in Eq (A7) has been correlated on the basis of our measurements due to lack of appropriate expressions for this coefficient.

To calculate the liquid flow rate Q_l (in the present case the water flow rate Q_w) contained in Eq (A2), the latter has been solved numerically using the Regula-Falshi method[13].

BOOK REVIEW

Forum on Unsteady Flow

Ed P. H. Rothe

This booklet documents the first of an anticipated series of forums on unsteady flow sponsored by the Fluid Transients Committee of the ASME Fluids Engineering Division. These forms mimic a highly successful series on cavitation sponsored by the Multiphase Flow and the Fluid Machinery Committees of the same Division, in which the opportunity is provided to present and discuss the current status of research projects before they are mature enough for publication in archival journals. As a result, this booklet is a collection of brief papers without in-depth introductions or, in many cases, complete conclusions.

Seventeen papers are organized into three major topics: I. Devices and systems affected by unsteady flow; II. Unsteady flow in piping: III. Basic studies and reviews of unsteady flows. The six papers in the first topic address such diverse devices and systems as wave rotors, MHD channel flow, wing/plate junction flow, propellant sloshing, and water hammer. Several papers describe analytical studies while others are experimental.

The six papers in the area of unsteady flow in piping represent the largest number addressing a single unsteady flow topic. Included is a diversity of piping related problems from a 'Case of feedwater piping vibration' to the analysis of the unsteady flow of non-Newtonian fluids and a Bingham plastic. Topic III includes three papers concerning unsteady convective heat transfer. One of these entitled 'Convective heat transfer enhancement in unsteady channel flow—a review', not only provides a good introduction to the subject, but also an extensive bibliography.

Although the papers are brief and diverse, the booklet serves to introduce some current research problems in unsteady flow. It is hoped that this sort of forum will expand in the future and provide the thermal sciences community with a valuable insight to the complex phenomena associated with unsteady flows. The efforts of the Editor and authors are applauded.

R. E. Henderson
Garfield Thomas Water Tunnel,
The Pennsylvania State University,
USA

Published, price $18.00, by ASME, 345 East 47th Street, New York, NY 10017, USA. (ASME code FED—vol. 16)